Effect of Tilt-Angle on Electron Tunneling through Organic Monolayer Films

H. Yamamoto and D. H. Waldeck*

Chemistry Department, University of Pittsburgh, Pittsburgh, Pennsylvania 15260

Received: December 19, 2001; In Final Form: March 16, 2002

This work explores how the geometry of alkanethiol molecules in organic thin films impacts the tunneling of electrons from an electrode to a redox species in solution. Film thicknesses for $C_8H_{17}SH$ (C8), $C_{12}H_{25}SH$ (C12), and $C_{16}H_{33}SH$ (C16) self-assembled monolayers (SAMs) on InP(100) were determined by angle-resolved X-ray photoelectron spectroscopy to be 6.4 ± 0.7, 11.1 ± 0.6, and 14.9 ± 1.2 Å, respectively. These thicknesses correspond to tilt-angles of 62 ± 4° for C8, 53 ± 3° for C12, and 51 ± 4° for C16 SAMs, which gives an average tilt-angle of 55 ± 6°. The decay constants for electron tunneling through alkanethiols on InP(100), Au(111), and Hg(liquid) are shown to correlate with the geometry, "tilt" angle, of the alkane chains on the surface. This work suggests that superexchange coupling between the alkane chains, which comprise the insulating film, can play an important role in defining electron tunneling barriers, especially for highly tilted chains.

Introduction

Self-assembled monolayer (SAM) films, composed of alkanethiols, form highly insulating tunneling barriers on the surface of metal and semiconductor electrodes.[1,2] The electron-transfer rate constant k_{ET} displays an exponential dependence on the length of the alkane chain,

$$k_{ET} \propto \exp(-\beta_n \cdot n) \tag{1}$$

where n is the number of methylene units in the chain and β_n is a tunneling decay constant per methylene unit. Although a number of workers have used these films to investigate fundamental aspects of electron transfer to redox species in solution, a number of issues still remain, e.g., deviation from an exponential distance dependence for short alkanethiol SAMs[3] and a structural dependence for the electron tunneling pathways.[4−10] This study addresses the importance of the tilt-angle of alkane chains on the electron tunneling efficiency.

The current work investigates electron transfer in the thick film/nonadiabatic limit. For electron reduction, the rate constant k_{red}^{NA} is given by

$$k_{red}^{NA}(\eta) = \int \rho(\epsilon) \cdot f(\epsilon) \cdot D_{ox}(\epsilon,\lambda,\eta) \cdot P(\epsilon,\eta) \cdot d\epsilon \tag{2}$$

where the integral is taken over the electronic energy ϵ. The available electronic states in the electrode are determined by the density of states $\rho(\epsilon)$ and the Fermi-Dirac distribution law f(ϵ). $D_{ox}(\epsilon,\lambda,\eta)$ describes the density of electron accepting levels (for an oxidation reaction it would be the density of electron donating levels), and P(ϵ,η) is the tunneling probability. Using the classical Marcus model, one can write

$$k_{red}^{NA}(\eta) = \frac{2\pi}{\hbar} |V|^2 \frac{1}{\sqrt{4\pi\lambda k_B T}} \int_{-\infty}^{\infty} \rho(\epsilon) \cdot f(\epsilon) \cdot \exp\left[-\left(\frac{(\lambda + (\epsilon_F - \epsilon) + e\eta)^2}{4\lambda k_B T} \right) \right] \cdot d\epsilon \tag{3}$$

where ϵ_F is the Fermi energy for an electron in the electrode, λ is the reorganization energy, η is the overpotential, and $|V|$ is the magnitude of the electronic coupling between the redox species and the electrode. Although the reorganization energy changes with distance from the electrode surface, for the large distances discussed here the dominant distance dependent term is the electronic coupling |V|. The electronic coupling through alkane monolayer films is well-characterized by an exponential decay law,

$$|V| = |V_0| \cdot \exp(-\beta d/2) \tag{4}$$

where β is a decay constant and d is the physical thickness of the film along the surface normal. This distance dependence is responsible for the observed exponential distance dependence of the electron-transfer rate constant (see eq 1). The exponential decay of the electron-transfer rate constant and its viscosity independence provide useful experimental signatures for the nonadiabatic regime.[3]

The role of superexchange coupling pathways between alkane chains in ultrathin films has been investigated for structures in which the redox couple is covalently linked to the film. Finklea et al.[4] investigated systems with a set of different structures containing covalent and noncovalent contacts at the surface. They found that interchain coupling was a small contributor when the redox couple was exposed to the solution outside the film, but that interchain coupling was important when the redox couple was buried in the film. For a system where the redox couple is exposed to the solution, Napper et al.[5] showed that the replacement of a methylene unit in the alkane chain with an ether link caused a 4- to 5-fold reduction in the rate constant. Their study suggests that interchain coupling plays a minor role, compared with "through bond" coupling pathways, when the redox couple is covalently tethered. In contrast to this finding, Sumner et al.[6] have reported that electron tunneling through SAMs composed of methylenes and a carboamide moiety is not greatly different from that containing only a methylene moiety. These studies indicated that the interchain coupling depends on the position of the redox couple and the chemical composition of the chain.

* Corresponding author. E-mail: dave@pitt.edu.

10.1021/jp014612x CCC: $22.00
Published on Web 07/03/2002

Systems in which the redox couple is not tethered display a similar range of behavior. Cheng et al.[7] studied the system of hydroxyl-terminated alkanethiols, and reported that the electron-transfer rate through the film is reduced by the introduction of ether moieties into the alkane chain, in agreement with the finding of Napper,[5] and is even further reduced by the presence of a conjugated unit, an alkyne functionality. On the other hand, Sek et al.[8] reported enhancement of the electron-transfer rate for alkanethiol chains that contain an amide moiety, both for a tethered redox species and an untethered redox couple. They ascribed the increase in the interchain superexchange interaction as arising from a hydrogen bond network that links the chains together.

Slowinski et al.[9] recently proposed a model in which the electron tunneling proceeds by both "through bond" and "through space" pathways. The model accounted for the film thickness dependence of electron tunneling through alkanethiol SAMs on a Hg droplet for which they could systematically vary the tilt-angle of the chains. This study extends their model[9] to explain the apparent change in the tunneling decay parameter found on different alkanethiol-coated electrode (Hg, Au, and InP) systems. This work reports the tilt-angles of alkanethiols on InP(100) determined by angle-resolved X-ray photoelectron spectroscopy, and combines this information with previously reported data to explain the relationship between the tilt-angles and the electron tunneling decay constants.

Experimental Section

A wafer of InP(100) (Crystacomm, with a dopant density of 1.3×10^{16} cm^{-3}) was used in these studies. Reagent grade $C_8H_{17}SH$, $C_{12}H_{25}SH$, and $C_{16}H_{33}SH$ were purchased from Aldrich and used without further purification. $C_8H_{17}SH$, $C_{12}H_{25}$-SH, and $C_{16}H_{33}SH$ are hereafter referred to as C8, C12, and C16, respectively. The alkanethiol-based SAMs were prepared on the surface of InP in the manner described previously[10] and were found to show high contact angles with water (110 ° for C8, 114 ° for C12, and 112 ° for C16).

Attenuation of the In $3d_{5/2}$ core level peaks as a function of the surface's takeoff angle, θ, was measured for C8, C12, and C16 layers. These data were normalized to the peak intensity of an Ar^+-sputtered clean InP,[11] corrected for the instrumental factor,[12] and analyzed with the least-squares method. Average tilt-angles of the SAMs before and after correction were 54.3° and 55.2°, respectively. The XPS apparatus was a Physical Electronics model 550, which contains a cylindrical, double-pass energy analyzer and a Mg Kα X-ray source, 1253.6 eV radiation. The energy resolution for the apparatus was determined to be about 1 eV, by calibration with the Fermi edge of sputter-cleaned rhodium. The base pressure in the apparatus was $1-3 \times 10^{-9}$ Torr during measurements on the SAM-coated InP. The details of the ARXPS measurement and instrument were reported elsewhere.[11]

The molecular lengths for the alkanethiols, as discussed later, were calculated as the distance between the H of the methyl and the S on the molecule's other end using GaussView 2.1. Hartree-Fock calculations with geometry optimization were performed at the 3-21G level. A value of 2 Å was added to account for the distance between the end S of the alkanethiols and the substrate.[13]

Tilt-Angle Determination

The thickness of the films was determined from angle-resolved X-ray photoelectron spectra, using the following equation:[14]

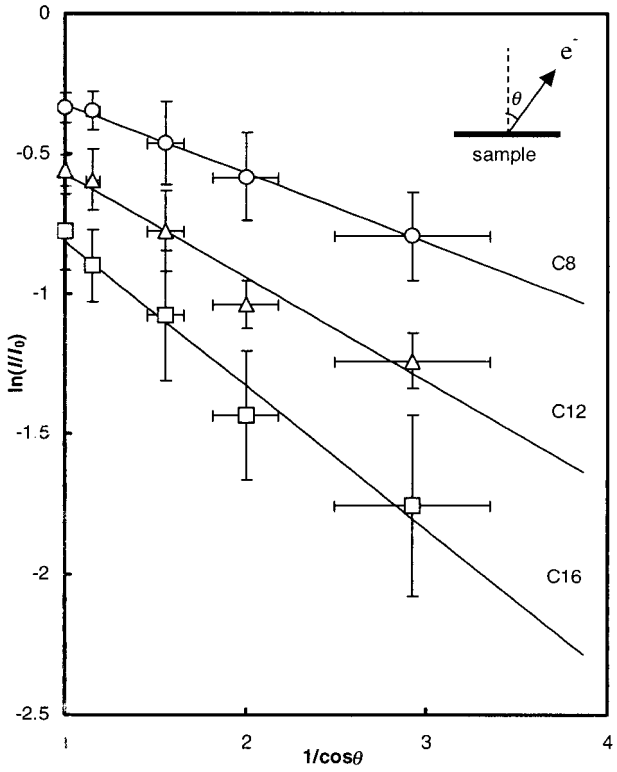

Figure 1. Attenuation curves for the In $3d_{5/2}$ core levels through the C8 (○), C12(△), and C16 (□) self-assembled monolayers. The inset illustrates the geometry in the ARXPS measurement.

$$\ln\left(\frac{I(\theta)}{I_c(\theta)}\right) = -\frac{d}{\lambda \cdot \cos(\theta)} \qquad (5)$$

where $I(\theta)$ is the photoelectron intensity from the substrate covered by the thin film, $I_c(\theta)$ is the photoelectron intensity from the clean substrate, θ is the angle of the detector with respect to the surface normal, d is the thickness of the film, and λ is the attenuation length of photoelectrons from the substrate. The inset of Figure 1 illustrates the experimental geometry. Equation 5 predicts that a plot of $\ln[I(\theta)/I_c(\theta)]$ versus $1/\cos\theta$ should be linear with a slope of $-(d/\lambda)$. The attenuation length λ was determined to be 26.7 Å for photoelectrons with a kinetic energy of 805.4 eV from the In $3d_{5/2}$ core level through *n*-alkanethiols.[11] Figure 1 shows plots for the attenuation of the In $3d_{5/2}$ core levels through the C8, C12, and C16 SAMs. The thicknesses of C8 (6.4 ± 0.7 Å), C12 (11.1 ± 0.6 Å), and C16 (14.9 ± 1.2 Å) SAMs were determined from the slopes of the best fit lines shown in Figure 1. Molecular lengths for the alkanethiols were determined to be 13.4 Å for C8, 18.5 Å for C12, and 23.6 Å for C16 SAM, as described in the Experimental Section. From the molecular lengths and the physical thicknesses, the tilt-angles of C8, C12, and C16 SAMs were found to be 62 ± 4, 53 ± 3, and 51 ± 4°, respectively. An average tilt-angle of 55 ± 6 ° will be used in the later discussion.

The tilt-angle of the SAM depends on the details of the substrate and the packing. For example, tilt-angles of alkanethiols are reported to be ∼5° on Au(100), ∼30° on Au(111),[2a,15] 0−14° on Ag(111),[2a,16] 57° on GaAs(100),[17] and ∼0° on Hg (liquid) which was estimated from the observed film thicknesses of 17.5 Å for C12 and 25.0 Å for C18.[18,19] The average tilt-angle of 55° for InP (100) is reasonable when compared with that of 57° reported for GaAs (100), since the lattice constant

TABLE 1: Measured and Calculated Tilt-Angles of Alkanethiols on Au(100), Au(111), Ag(111), GaAs(100), InP(100), and Hg(liquid)

	S−S distance	measured tilt-angle	tilt-angle: method 1[c]	tilt-angle: method 2[d]	
Au(100)	4.54 [2a]	∼5 [2,15]	14	0	0
Au(111)	4.92 [2a]	26−28 [2,15]	28	18	0
Ag(111)	4.6−4.7[2a]	0−7 [2,16]	19	0	0
GaAs(100)	5.653[a]	57 [17]	39	43	39
InP(100)	5.869[a]	55	41	47	44
Hg(liquid)	3.610[b]	∼0[9]	0	0	0

[a] The sulfurs are assumed to be in the hollow of the (100) or (111) lattice. [b] The sulfurs are assumed to have the Hg−Hg distance of 3.61 Å [c] Tilt-angle = $\cos^{-1}$(4.4 /S−S distance). The tilt-angle for Hg is taken to be 0° because the S−S distance is shorter than the 4.4 Å, the chain-to-chain distance in method 1. [d] The left column is tilt-angle = $\cos^{-1}$(18.4 Å^2/(π × (S−S distance/2)^2)) [ref 2b], whereas the right column is tilt-angle = $\cos^{-1}$(19.5 Å^2/(π × (S−S distance/2)^2)) [ref 9]. The tilt-angles for Au(100), Ag(111), and Hg(liquid) are taken to be 0° because the S−S distances are shorter than the 4.84 Å [ref 2b] or 4.98 Å [ref 9], the chain-to-chain distance in method 2.

of 5.869 Å for InP (100) is comparable to that of 5.563 Å for GaAs (100).[20] Ulman has discussed the tilt-angles of alkanethiol SAMs on Au, Ag, and GaAs in terms of the chain-to-chain packing distance and the S−S distance at the surface.[2a] Ulman suggests using a chain-to-chain distance of 4.4 Å, determined for a trigonal lattice of SAMs, to describe the chain packing.[21] On the other hand, Schreiber[2b] has discussed packing of alkanethiol SAMs on Au in terms of the area each molecule occupies, as compared to the cross-sectional area of 18.4 Å^2 for the molecule. Slowinski[9] suggested another cross-sectional area of 19.5 Å^2. Table 1 lists the S−S distances along with the measured and calculated tilt-angles for alkanethiols on Au(100), Au(111), Ag(111), GaAs(100), InP(100), and Hg(liquid). These calculations assume that S−S distances are commensurate with the lattice spacing of the substrates. The tilt-angles were calculated using the two methods described above, the chain-to-chain method (method 1) and the area method (method 2). As can be seen in Table 1, the calculated tilt-angles are qualitatively in agreement with the measured ones.

Electron Tunneling

Slowinski et al.[9] found a tilt-angle dependence for electron transfer through alkanethiol SAMs on Hg electrodes, and proposed a two pathway model to account for this dependence. One pathway is the "through bond" superexchange along a chain and the second pathway involves "through bond" superexchange but includes a single interchain superexchange hop. The tunneling current from this treatment is given by[9]

$$I_t = I_0 \exp(-\beta_{tb} L_M) + I_0 n_s \exp(-\beta_{tb}(L_M - d_{cc} \tan\theta)) \times \exp(-\beta_{ts} d_{cc}) \quad (6)$$

where I_t is the tunneling current through the SAM, β_{tb} is the decay constant for "through bond" tunneling, and β_{ts} is the tunneling constant for "interchain" tunneling. The other parameters in eq 6 are the molecular length L_M, the chain-to-chain distance d_{cc} (= 4.98 Å), the tilt-angle θ, and a statistical factor n_s, which accounts for the increased number of pathways when interchain hopping is allowed. For the dodecanethiol system, Slowinski et al.[9] determined that β_{tb} = 0.91 Å^{-1} and β_{ts} = 1.31 Å^{-1} when n_s was assumed to be the same as the number of carbons in the alkane chain.[9] Figure 2 shows the logarithm of the normalized tunneling current (broken line) as a function of the tilt-angle that is predicted by eq 6. Here, "the normalized tunneling current" is defined to be the ratio of the tunneling current through alkane chains comprised of twelve methylenes (I_t) to the current without the SAM (I_0). I_0 is determined separately for each electrode system (Au, Hg, and InP) by extrapolation from the observed current for twelve methylenes back to the case of zero methylenes using the experimentally observed tunneling decay constant β_n, reported in Table 2. The broken curve, which represents the single interchain hopping model, provides reasonable agreement with the data for Hg and Au. However, it does not adequately describe the InP data at high tilt-angle.

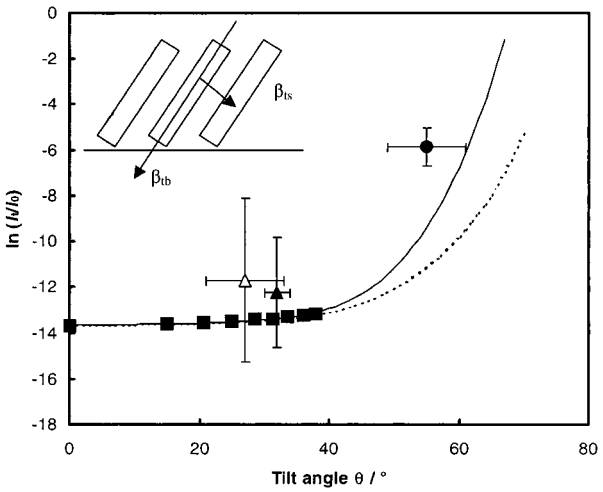

Figure 2. The normalized tunneling current is plotted as a function of the tilt-angle of a dodecanethiol self-assembled monolayer on Hg (■), InP (●), and Au (▲; dodecanethiol, △; hydroxy-terminated dodecanethiol) electrodes. The normalized currents for the electrode systems were obtained from the measured β_n via the equation $-\beta_n n_c$, where n_c = 12 (see Table 2). The calculated tunneling current when one interchain hop is allowed in the superexchange pathway is indicated with the broken line, and the tunneling current for which up to two interchain hops are allowed in the superexchange pathway are shown by the solid line.

A model that allows for multiple interchain hops provides a better description of the observed tunneling current at high angles. For N interchain hops in the superexchange pathways, the distance for a "through bond" tunneling contribution along the chain tilted at angle θ is reduced by (Nd_{cc} tan θ), while the distance for "through space" hopping is given to be Nd_{cc}. Hence, at large angles, the effective distance can be significantly shorter when interchain hops are included. In addition, the number of pathways grows with the number of interchain hops. Including N interchain pathways gives a total tunneling current I_t of

$$I_t = I_0 \exp(-\beta_{tb} L_M) + I_0 \sum_{N=1}^{\frac{L_M \cos\theta}{d_{cc}}} \frac{n_s!}{(n_s - N)!N!} \exp(-\beta_{tb}(L_M - N d_{cc} \tan\theta)) \times \exp(-\beta_{ts} N d_{cc}) \quad (7)$$

In this sum, the number of interchain hops is constrained by the fact that $N \le L_M \cos\theta / d_{cc}$, since the total distance Nd_{cc} of "through space" hops cannot exceed the film thickness $L_M \cos\theta$. The solid curve in Figure 2 shows the normalized tunneling current (solid line) as a function of tilt-angle, as predicted by eq 7 for a C12 chain. At small angles, the broken curve, eq 6, agrees with the solid curve found from eq 7. At high angle, the solid curve with multiple interchain hopping

TABLE 2: Tunneling Decay Constants per Methylene Unit, the Logarithm of Normalized Tunneling Currents through a C12 SAM, and Tilt-Angles of the SAM for Different Systems

system	β_n (per CH_2)	$\ln(I_t/I_0)$	tilt-angle/°
Hg/Cl2	1.14 ± 0.09 [9]	-13.68 ± 1.08	16 ± 12[a]
Au(111)/C12	1.02 ± 0.20 [22]	-12.24 ± 2.40	32 ± 2 [23]
Au(111)/C13OH[b]	0.90 ± 0.30 [24a]	-11.70 ± 3.60	27 ± 6 [24b]
InP(100)/C12	0.49 ± 0.07 [10]	-5.88 ± 0.84	55 ± 6

[a] The tilt-angle was estimated from the molecular area of 20.3 ± 2.1 Å^2/molecule for C12 in ref 9. [b] The tunneling distance through hydroxy-terminated dodecanethiol have been reported to be smaller by about one methylene chain than that through dodecanethiol (see refs 9 and 24).

current shows a stronger angle dependence than the broken curve with only a single interchain hopping. This result indicates that the contribution of the multiple interchain hopping pathways to tunneling current becomes more important at high tilt-angle.

Figure 2 plots the experimental points of the normalized tunneling current for a C12 SAM that are obtained from the tunneling decay constant β_n, as reported for Hg(liquid),[9] Au(111),[3,22−24] and InP(100).[10] Table 2 presents the decay constants per methylene unit and the normalized tunneling currents. In these data, the observed tunneling current I_t through twelve methylenes is divided by the current for tunneling through zero methylenes, I_0, for each experimental system. This normalization procedure should correct for many of the differences between the different systems, such as reorganization energy, reaction free energy, and density of electronic states in the electrode,[25,26] as long as the electron-transfer mechanism remains in the nonadiabatic limit.[3] However, this analysis does not account for all of the differences between the experimental systems. In particular, differences in the distance dependence of the electronic states for the different electrode materials (Hg, Au, and InP) could cause changes in the characteristic decay length that is observed for tunneling.[27]

This effect can be addressed by using a tunneling barrier model for the SAM layer on the electrode. For example, as the height of the "effective" tunneling barrier becomes larger, the electronic wave functions of the electrodes will decay faster. In the simple limit, the height of the "effective" tunneling barrier will scale with the Fermi energy of the electron in the metal systems and the valence band edge in the InP system.[10,27] The work function of Au is about 5.3 eV and that of Hg is 4.5 eV.[20] The valence band edge for InP is somewhat more difficult to identify, but it can be placed near 5.8 eV on the vacuum scale.[28] On a qualitative level, this shift in the electron energetics between the systems (Hg to Au to InP) is consistent with the trend in tunneling decay constant, assuming that the electron-transfer proceeds through hole mediated superexchange.[5] However, a quantitative analysis of these data requires that the tunneling barrier be unrealistically small and implies that the offset between the hole superexchange levels of the insulating layer and the valence band edge of InP be only 0.3 eV.[29] Simple theoretical treatments of the superexchange mechanism for hole mediated superexchange suggest that the energy effect should be weak for systems in which the tunneling energy lies nearly midway between the HOMO and LUMO states of the bridge material,[30] as is the case for alkanethiols on these electrode materials.

As can be seen in Figure 2, the experimental data are in good agreement with the calculated curve when both one- and double-interchain hops are included into the tunneling current calculation, especially at high tilt-angles. Although tunneling energy effects may contribute in these systems, the analysis suggests that it is not the major factor. Hence, the tunneling current found for the InP system, which has highly tilted chains, can be understood by consideration of the multiple hopping superexchange pathways.

In summary, it is found that the thickness dependence of the electron transfer rate constant from an electrode, through an alkanethiol SAM, to a freely diffusing redox couple in solution changes in a systematic manner between Hg, Au, and InP electrodes. The differences found in the observed thickness dependences appear to be correlated with the tilt-angle of the alkane chains in the film. The analysis indicates that the geometry of the alkane chains plays an important role in defining electron tunneling barriers, and that interchain couplings become important for highly tilted alkane chains.

Acknowledgment. We thank the Department of Energy (DE-FG02-89ER14062) for support of this work.

References and Notes

(1) Finklea, H. O. *Electroanalytical Chemistry*; Bard, A. J., Rubinstein, I., Eds.; Marcel Dekker: New York, 1996; *Vol. 19*, 109; (b) Miller, C. J. *Physical Electrochemistry: Principles, Methods and Applications*; Rubinstein, I., Ed.; Marcel Dekker: New York, 1995; 27.

(2) Ulman, A. *Chem. Rev.* **1996**, *96*, 1533; (b) Schreiber, F. *Prog. Surf. Sci*. **2000**, *65*, 151. (c) Nuzzo, R. G.; Korenic, E. M.; Dubois, L. H. *J. Chem. Phys.* **1990**, *93*, 767; (d) Forster, R. J.; Faulkner, L. R. *J. Am. Chem. Soc.* **1994**, *116*, 5453; (e) Smalley, J. F.; Feldberg, S. W.; Chidsey, C. E. D.; Linford, M. R.; Newton, M. D.; Liu, Y.-P. *J. Phys. Chem.* **1995**, *99*, 13141; (f) Avila, A.; Gregory, B. W.; Niki, K.; Cotton, T. M. *J. Phys. Chem. B* **2000**, *104*, 2759; (g) Feng, Z. Q.; Imabayashi, S.; Kakiuchi, T.; Niki, K. *J. Chem. Soc., Faraday Trans.* **1997**, *93*, 1367.

(3) Khoshtariya, D. E.; Dolidze, T. D.; Zusman, L. D.; Waldeck, D. H. *J. Phys. Chem. A* **2001**, *105*, 1818.

(4) Finklea, H. O.; Liu, L.; Ravenscroft, M. S.; Punturi, S. *J. Phys. Chem.* **1996**, *100*, 18852.

(5) Napper, A. M.; Liu, H.; Waldeck, D. H. *J. Phys. Chem. B* **2001**, *105*, 7699.

(6) Sumner, J. J.; Weber, K. S.; Hockett, L. A.; Creager, S. E. *J. Phys. Chem. B* **2000**, *104*, 7449.

(7) Cheng, J.; Saghi-Szabo, G.; Tossell, J. A.; Miller, C. J. *J. Am. Chem. Soc.* **1996**, *118*, 680.

(8) Sek, S.; Misicka, A.; Bilewicz, R. *J. Phys. Chem. B* **2000**, *104*, 5399. (b) Sek, S.; Bilewicz, R. *J. Electroanal. Chem.* **2001**, *509*, 11.

(9) Slowinski, K.; Chamberlain, R. V.; Miller, C. J.; Majda, M, *J. Am. Chem. Soc.* **1997**, *119*, 11910.

(10) Gu, Y.; Lin, Z.; Butera, R. A.; Smentkowski, V. S.; Waldeck, D. H. *Langmuir* **1995**, *11*, 1849. (b) Gu, Y.; Waldeck, D. H. *J. Phys. Chem.* **1998**, *102*, 9015.

(11) Yamamoto, H.; Gu, Y.; Butera, R. A.; Waldeck, D. H. *Langmuir* **1999**, *15*, 8640.

(12) Because the instrumental factor for clean InP was different from that for the SAMs, the intensity for clean InP was corrected. The intensity in terms of $1/\cos\theta$ was simulated using an exponential function. The exponential decay constant was changed in order to give straight lines for C16, C12, and C8. See ref 14 for a general discussion of this procedure.

(13) Smalley, J. F.; Feldberg, S. W.; Chidsey, C. E. D.; Linford, M. R.; Newton, M. D.; Liu, Y.-P. *J. Phys. Chem.* **1995**, *99*, 13141.

(14) Hofmann, S. Depth Profiling in AES and XPS. From *PRACTICAL SURFACE ANALYSIS*; Briggs, D., Seah, M. P., Eds.; Wiley: Chichester, New York, Brisbane, Toronto, Singapore, 1996.

(15) Porter, M. D.; Bright, T. B.; Allara, D. L.; Chidsey, C. E. D. *J. Am. Chem. Soc.* **1987**, *109*, 3559. (b) Kondo, T.; Yanagida, M.; Shimazu, K.; Uosaki, K. *Langmuir* **1998**, *14*, 5656.

(16) Ulman, A. *J. Mater. Educ.* **1989**, *11*, 205. (b) Laibinis, P. E.; Whitesides, G. M.; Allara, D. L.; Tao, Y.-T.; Parikh, A. N.; Nuzzo, R. G. *J. Am. Chem. Soc.* **1991**, *113*, 7152. (c) Nemetz, A.; Fischer, T.; Ulman, A.; Knoll, W. *J. Chem. Phys.* **1993**, *98*, 5912.

(17) Sheen, C. W.; Shi, J. X.; Martensson, J.; Parikh, A. N.; Allara, D. L. *J. Am. Chem. Soc.* **1992**, *114*, 1514.

(18) Haag, R.; Rampi, M. A.; Holmlin, R. E.; Whitesides, G. M. *J. Am. Chem. Soc.* **1999**, *121*, 7895.

(19) Magnussen, O. M.; Ocko, B. M.; Deutsch, M.; Regan, M. J.; Pershan, P. S.; Abernathy, D.; Gruebel, G.; Legrand, J.-F. *Nature* **1996**, *384*, 250−252.

(20) *CRC Handbook of Chemistry and Physics*; Lide, D. R., Ed.; CRC: Boca Raton, Ann Arbor, London, Tokyo, 1994.

(21) Ulman, A.; Eilers, J. E.; Tillman, N. *Langmuir* **1989**, *5*, 1147.

(22) Xu, J.; Li, H.-L.; Zhang, Y. *J. Phy. Chem.* **1993**, *97*, 11497.

(23) Dubois, L. H.; Nuzzo, R. G. *Annu. Rev. Phys. Chem.* **1992**, *43*, 437. (b) Fenter, P.; Eberhardt, A.; Liang, K. S.; Eisenberger, P. *J. Chem. Phys*. **1997**, *106*, 1600.

(24) Miller, C.; Cuendet, P.; Grätzel, M. *J. Phys. Chem.* **1991**, *95*, 877. (b) Sinniah, K.; Cheng, J.; Terrettaz, S.; Reutt-Robey, J. E.; Miller, C. J. *J. Phys. Chem*. **1995**, *99*, 14500.

(25) Gosavi, S.; Marcus, R. A. *J. Phys. Chem. B* **2000**, *104*, 2067; (b) Gao, Y. Q.; Georgievskii, Y.; Marcus, R. A. *J. Chem. Phys*. **2000**, *112*, 3358.

(26) Pomykal, K. E.; Fajardo, A. M.; Lewis, N. S. *J. Phys. Chem.* **1996**, *100*, 3652; (b) Royea, W. J.; Fajardo, A. M.; Lewis, N. S. *J. Phys. Chem. B* **1997**, *101*, 11152; (c) Lewis, N. S. Annu. Rev. Phys. Chem. **1991**, *42*, 543.

(27) Gu, Y.; Waldeck, D. H. *J. Phys. Chem.* **1996**, *100*, 9573.

(28) Tan, M. X.; Laibinis, P. E.; Nguyen, S. T.; Kesselman, J. M.; Stanton, C. E.; Lewis, N. S. *Prog. Inorg. Chem.* **1994**, *41*.

(29) Background on this argument is developed in ref 10b and finds that $\beta = 1.024\sqrt{E_{\text{bridge}}-E}$, where we have written the tunneling barrier as the difference between the tunneling energy E and the energy of bridge superexchange states E_{bridge} (which should correspond to the cation states of the bridge for hole mediated superexchange and is given by the ionization potential of the alkane, approximately). Comparisons of the data in Table 2 with the energies given in the text indicate that E_{bridge} must lie between 6.1 and 6.2 eV. No other evidence exists to support such a low ionization potential for alkane chains.

(30) Beratan, D. N.; Onuchic, J. N. *Adv. Chem.* **1991**, *228*, 71.